Author/s:
Yuan, R;Kennedy, DM;Stephenson, WJ;Gómez-Pujol, L

Title:
Experimental investigations into the influence of biofilms and environmental factors on short-term microtopographic fluctuations of supratidal sandstone

Date:
2019-06-15

Citation:
Yuan, R., Kennedy, D. M., Stephenson, W. J. & Gómez-Pujol, L. (2019). Experimental investigations into the influence of biofilms and environmental factors on short-term microtopographic fluctuations of supratidal sandstone. Earth Surface Processes and Landforms, 44 (7), pp.1377-1389. https://doi.org/10.1002/esp.4581.

Yuan Runjie (Orcid ID: 0000-0002-3099-8970)
KENNEDY DAVID (Orcid ID: 0000-0002-4878-7717)
Stephenson Wayne (Orcid ID: 0000-0002-4020-5639)

Experimental investigations into the influence of biofilms and environmental factors on short-term microtopographic fluctuations of supratidal sandstone

Runjie Yuan,[1]* David M. Kennedy,[1] Wayne J. Stephenson[2] and Lluís Gómez-Pujol[3]

[1] School of Geography, The University of Melbourne, Parkville Vic 3010, Australia

[2] Department of Geography, The University of Otago, Dunedin, New Zealand

[3] Earth Sciences Research Group, Department of Biology, Universitat de les Illes Balears, Cra. Valldemossa km 7.5, 07122 Palma (Balearic Islands), Spain

* Corresponding Author, runjiey@student.unimelb.edu.au, +61 3 8344 9168

This is the author manuscript accepted for publication and has undergone full peer review but has not been through the copyediting, typesetting, pagination and proofreading process, which may lead to differences between this version and the Version of Record. Please cite this article as doi: 10.1002/esp.4581

Abstract

In this study laboratory experiments were used to explore the role of biofilms, formed by lithobiontic microorganism communities, in causing hourly surface changes of supratidal sandstone and the potential linkage to long-term rock decay. To isolate the influence of individual environmental factors (temperature and humidity) on rock surface changes (expansion and contraction), a colonized (biofilm-covered) and a non-colonized sandstone block (biofilm-free) underwent the same univariate microclimatic simulations closely controlled by an environmental chamber. Simulations were run under three different light conditions, with a natural light lamp on, on and off at 20-minute intervals and off, to investigate the impact of light on rock surface dynamics. Measured with a traversing micro-erosion meter (TMEM), 2-hourly microtopographic fluctuations of these two sandstone blocks were compared in the same environment. Induced by microclimatic variations, surface movements of significantly higher magnitude (12 - 120% under varying tempeature and 121 - 154% under varying humidity) and different change patterns were observed on the colonized block, indicating the primary role of biofilm in driving microtopographic fluctuations of supratidal sandstone. However, thermally driven changes of similar magnitude and pattern were observed on both surfaces, suggesting other mechanisms also operating on the non-colonized rock surface in this process. Due to the sensitivity of biofilm microorganism communities to light, the magnitude and pattern of surface changes was impacted by light condition. Because biofilms increased the magnitude and number of cycles of expansion and contraction of the experimental rock surface, we propose lithobiontic biofilms facilitate the detachment of grains and granular disintegration on the rock surface, consequently contributing to rock decay and accelerating the rate of

breakdown of supratidal rock. This short-term episode therefore needs to be superimposed on longer term studies to fully understand the role of biofilms in rock surface change.

KEYWORDS: laboratory simulation; traversing micro-erosion meter; biogeomorphology; rock decay; rocky coast

Introduction

The micro-erosion meter (MEM) (High and Hannah, 1970) and the adapted traversing micro-erosion meter (TMEM) (Trudgill *et al.*, 1981) have been widely used on rocky coasts to measure erosion rates on shore platforms (for a review see Stephenson and Finlayson, 2009). Data derived from these instruments have demonstrated that coastal rock surfaces are dynamic at millimetre to centimetre scales with expansion and contraction of bedrock occurring over a range of time scales (Kirk, 1977; Mottershead, 1989; Stephenson and Kirk, 2001; Taylor, 2003; Stephenson *et al.*, 2004; Swantesson *et al.*, 2006; Foote *et al.*, 2006; Porter and Trenhaile, 2007). The expansion of rock surfaces, generally ranging from 0.01 to 1 mm in the vertical plane, often procures granular disintegration by generating stress in rock bodies (Stephenson and Kirk, 1996; Porter *et al.*, 2010). This granular-scale erosion is of particular significance in the lowering of shore platforms formed in homogenous bedrock where widely spaced joints inhibit direct wave plucking of blocks (Naylor and Stephenson, 2010; Trenhaile and Porter, 2018).

Recently, a number of field studies making measurements at hourly scale have been conducted on a variety of lithologies to identify drivers of these microtopographic changes and better understand rock decay. On intertidal shore platforms, rocks experience cycles of exposure and inundation, and wetting and drying has been shown to be the main mechanism of short-term surface changes (Hemmingsen *et al.*, 2007; Porter and Trenhaile, 2007). However, these microtopographic fluctuations are also commonly observed on supratidal rocks which are only occasionally covered by marine inundation (Trenhaile, 2006; Gómez-Pujol *et al.*, 2007; Mayaud *et al.*, 2014). Alternate wetting and drying, therefore is less important for rock surface changes occurring in the supratidal zone. At Marengo, Australia, lithobiontic biofilm has been hypothesised to be a key in controlling the dynamic nature of surface changes on supratidal rocks (Gómez-Pujol *et al.*, 2007). In France and Canada, other mechanisms such as thermal stress and moisture uptake by clay minerals have been implicated in driving microtopographic fluctuations alongside biofilms (Trenhaile, 2006; Mayaud *et al.*, 2014). Quantifying the precise role of each driver is however difficult in the field due to the ubiquitous growth of lithobiontic biofilms in the supratidal zone and the variable microclimates encountered on rock surfaces. As the overlap of the range of surface movement magnitude across differing temporal scales, the short-term microtopographic change needs to be considered in monitoring the long-term microtopographic change (Stephenson *et al.*, 2004; Gómez-Pujol *et al.*, 2007). The causal relationship between the short- and long-term surface changes, *i.e.* if the short-term surface dynamics contributes to the development of long-term event by generating repetitive fatigue, however, has not been fully understood (Hall and Thorn, 2014).

Limitations of previous studies are that the role of biofilm has only been inferred based on the correlation between the magnitude of surface movements and diameter of hyphae in biofilms (Gómez-Pujol *et al.*, 2007), and environmental factors act simultaneously on short-term rock surface dynamics (Mayaud *et al.*, 2014). In this paper, by comparing 2-hourly microtopographic changes between a colonized and a non-colonized rock surface in a controlled environmental chamber, we aim to investigate: (i) the role of lithobiontic biofilm in rock surface changes; (ii) the influence of each environmental factor on the cycle of expansion and contraction on supratidal sandstone and (iii) the potential linkage between the short- and long-term surface changes.

Methodology

Rock samples

The bedrock of shore platforms and cliffs at Marengo, Victoria, Australia (38°47'S, 143°40'E) (Figure 1) are composed of well-sorted, fine-grained sandstone (2 to 4 phi) with a relatively low porosity (10.59 ± 1.17%) (Gómez-Pujol *et al.*, 2007), which is suitable for the colonization of lithnbiotic biofilms (Cockell *et al.*, 2018). The main components include volcanic fragments, quartz and clay minerals. With extensive colonization of lithobiontic biofilms on the rock surface, supratidal sandstones used in this study have been previously shown to be highly responsive to changes in microclimate and biofilm has been inferred as a key cause of rock surface changes (Gomez-Pujol *et al.*, 2007; Yuan *et al.*, 2018) so are suitable for our investigation. The test rock was collected from the same bed as used in the previous studies (Gomez-Pujol *et al.*, 2007; Yuan *et al.*, 2018) (Figure 2).

The block was cut into two pieces (200 - 300 × 180 - 260 × 80 - 100 mm), large enough to accommodate a TMEM bolt set. The weathered face of each block was relatively flat with a similar surface roughness and colonization indicated by the rock surface coloration, as well as by binocular loupe observations.

For the experiments one block was left in the same condition as collected in the field and the second cleaned of biofilms (Figure 3). The biofilm-free block was cleaned by oven drying at 90°C for 24 hours and then washed with H_2O_2 (8%) in order to eliminate biological cover and preserve the surface roughness (Leznicka *et al.*, 1988). The surface was then rinsed with running distilled water to clean off the remaining H_2O_2 and organic substances and air-dried naturally.

An equilateral triangle TMEM bolt set was then installed in each test face. The bolts used were 7 cm in length and 8 mm in diameter. They were cemented into the pre-drilled holes using fast curing polyester (Ramset Chemset 101). The length of the bolts and the strength of cement ensured that the bolts were not affected by the expansion and contraction of the rock surface due to the relatively low thermal expansion coefficient and thermal conductivity of sandstone (in the order of *c.*$10 \times 10^{-6}\ K^{-1}$ and 2 – 5 W m K^{-1}) (McKenna *et al*., 1996; NPL, 2010). Bolt sets were installed in the central part of the face to minimise edge effects (as per Porter and Trenhaile, 2007). The prepared blocks were placed into polystyrene cases separately, leaving the test faces exposed. This was not only to protect the blocks from possible damage during the course of experiments, but also to ensure conditions were as representative of larger rock masses by minimizing edge

effects and concentrating thermal exchange through the upper weathered faces (Gowell *et al.*, 2015).

Environmental conditions simulation

An environmental chamber (Associated Environmental Systems BHD-2003) was used to simulate environmental conditions representative of those measured at Marengo (in the middle of November) (Yuan *et al.*, 2018). To isolate the individual impact of air temperature and humidity, one variable was held constant while the second varied during simulations. For example, for temperature, a constant relative humidity of 75% was adopted which is the average value recorded in the field (Yuan *et al.*, 2018); while air temperature varied from 12 to 33°C. This range is close to the local daily minimum and maximum temperatures during November (BoM, 2016). The thermal profile commenced with a 2-hour period at 12°C to ensure the block to equilibrate with the simulated environment. It was subsequently followed by a heating period (2 to 8 hours) from 12 to 33°C and a cooling period (8 to 14 hours) dropping to 12°C (Figure 4(a)). Rock surface microtopography was measured every 2 hours from 2 to 14 hours, with a difference of 7°C between any two successive measurements. Likewise, a constant temperature and dynamic humidity were set in the simulation to study the impact of humidity, including a dampening period (2 to 8 hours) and a drying period (8 to 14 hours) (Figure 4(b)). Air temperature was set at 22°C, while relative humidity ranged gradually between 45% and 87%, with a difference of 14% between two successive measurements. Rock temperature

at the surface was monitored every 2 hours with an infrared thermometer before the TMEM measurement was conducted.

Physiological activity of biofilms on supratidal sandstone has been suggested to be affected by cloud cover (Yuan *et al.*, 2018). To test this theory, a 40 Watt natural light lamp was installed to emit light of certain spectrum for the physiology of biofilms and heat blocks directly by radiation, replicating the heating of rock by insolation (Coombes, 2011; Gowell *et al.*, 2015). Combined with the convection provided by heating system of the chamber, the rock surface temperature was determined both by the ambient air and rock thermal properties, as occurring in the field (Warke and Smith, 1998; Smith *et al.*, 2005). All simulations for temperature and humidity studies were run under three light conditions respectively. They are with (i) the lamp on, to simulate the sunny weather with no or little cloud cover; (ii) the lamp on and off at 20-minute intervals, to simulate short-term thermal variations on coastal rock surfaces under partly/mostly cloudy condition; and (iii) the lamp off, to simulate the nocturnal environment. Under each treatment, the light condition was simulated over the entire course of the procedure.

Experimentation occurring with one block at a time in a constant location is deemed to be more repeatable (Carter and Viles, 2004). Each block was placed in the same position in the chamber, with the same distance to vent, heater and light source. The block with biofilms was measured first so as to minimise the lag between field collection and laboratory experimentation in case the colonized biofilm cannot grow or exist in the laboratory environment. For practicality, blocks were taken out of chamber for measurement. An initial test prior to the experimentation indicated the rock surfaces

remained stable for 10 minutes outside the chamber, which allowed TMEM measurements to be taken (Gómez-Pujol, 2014). A detailed description of the TMEM method is provided by Trudgill *et al.* (1981).

The entire experimentation was conducted over 12 days from 9 to 20 February 2017, following the order listed in Table I. There was a 10-hour gap between any two successive experiments to eliminate the possible cumulative effect of the previous treatment on the following one. Ninety-three coordinates were measured in an area of 41.3 cm^2 on each test surface. Under 12 different treatments, a total number of 7812 readings (n = 2 rock types × 2 variables × 3 light conditions × 7 measurement sets × 93 individual measurement coordinates) were recorded (Table I). SURFER 13 (Golden Software LLC) was used to generate contour plots of 2-hourly rock surfaces (Kriging gridding method) and calculate volumetric changes on the rock surface using Simpson's 3/8 rule (Yuan *et al.*, 2018).

Results

Colonization of lithobiontic biofilms

The presence of lithobiontic biofilms was indicated by the colouration induced by the biofilms on rock surface (rather than covering thallus) (Figure 3(a)) and confirmed by SEM images on the colonized rock surface (Figure 5). Top-down views showed the extensive biofilm cover on rock surface, and detached rock fragments embedded by hyphae were also commonly observed (Figure 5(a) and (b)). Cross-sectional views showed the lithobiontic biofilms consisting of two parts: the eplithic organisms colonizing on the surface

and the endolithic organisms penetrating into the sandstone beneath, typically in the thickness of tens of microns (Figure 5(c), (d) and (e)).

Rock surface temperature

Generally, under varying air temperature (and constant humidity), rock surface temperature increased in the heating period (from 2 to 8 hours) and decreased in the following cooling period (from 8 to 14 hours), with less range from 12 to 29 °C comparing with air temperature (Figure 6(a) and (c)). Compared with the conditions under light (CTO, CTA, NTO and NTA), rock surface temperature tended to be lower when the lamp was off (CTF and NTF). During treatments for humidity study, as humidity varied with a constant air temperature, rock surface temperature was stable and equilibrated at 22°C regardless of light conditions (Figure 6(b) and (d)).

The magnitude of rock surface change

As per the method of Stephenson *et al.* (2004), TMEM readings greater than 0.01 mm (±0.01 mm) were classified as measureable changes and median values were used to measure the central tendency of hourly surface movements. Generally, two surfaces behaved differently in response to moisture variations (Table II). The colonized rock surface was relatively active with > 50% changes being measureable and median values ranging from -0.040 to +0.068 mm; while < 40% changes were measureable on the non-colonized rock surface, ranging from -0.012 to +0.024 mm on average. Under varying air

temperature, the difference in surface movement was obvious when the lamp was off (CTF/NTF).

The Friedman two-way analysis of variance (ANOVA) by ranks was used to assess if the microtopographic changes were significant under each treatment (Matthews, 1981). The relative height of each coordinate was ranked against the previous reading over each 2-hour interval. The null hypothesis, there was no significant variation in short-term microtopography, was rejected for each treatment (CTO [χ_r^2 = 178.71]; CTA [χ_r^2 = 180.69]; CTF [χ_r^2 = 230.43]; CHO [χ_r^2 = 131.87]; CHA [χ_r^2 = 129.94]; CHF [χ_r^2 = 108.73]; NTO [χ_r^2 = 273.17]; NTA [χ_r^2 = 156.64]; NTF [χ_r^2 = 288.76]; NHO [χ_r^2 = 349.41]; NHA [χ_r^2 = 279.33]; NHF [χ_r^2 = 144.77]; $P < 0.001$). Therefore, there were significant changes in microtopography over 2-hourly measurements under each treatment.

To compare rock surface behaviours between the two blocks, the independent sample *t*-test was used to assess if there were significant differences in mean elevation changes of the two surfaces under the same condition. Surface changes under the same environment were examined in 6 pairs (6 comparisons per pair) (Table III). The null hypothesis that there was no difference in the mean elevation change between two surfaces was rejected in 81% of cases (29/36). More cases were rejected in humidity experiments (16/18) than temperature experiments (13/18).

Absolute values of 2-hourly surface changes were used to represent the magnitude of surface movements because the direction, i.e. if the rock surface expands or contracts, was not considered. To compare the magnititude of 2-hourly rock surface changes between the two surfaces, the *t*-test was used again to assess if surface movements were

magnified or not by the colonization of biofilms on the sandstone (Table IV). Significant higher surface changes were observed on the colonized block in 4 out of 6 comparisons. This magnification was more prominent in response to moisture variations (121% and 154%) than thermal variations (12% and 120%). With the lamp on, small but significantly reduced surface movements were observed on the colonized block under varying temperature (CTO/NTO).

The pattern of rock surface change

To examine the homogeneity of microtopographic changes across the rock surface, the Wilcoxon matched-pair rank test was used for each treatment (15 comparisons per treatment) (Matthews, 1981). The null hypothesis that there was no difference was rejected in 88% of cases (158/180), i.e. the rock surface tended to move as a heterogeneous body under all treatments.

The heterogeneity of surface changes was also identified by the commonly observed distinct 'hotspots' of expansion and contraction (small areas representing obvious surface movements) on both blocks, while rock surfaces tended to remain stable homogeneously across the entire surface (Figure 7). Under varying air temperature, the colonized rock surface mainly contracted during the heating period and expanded during the cooling period. This pattern was particularly obvious under CTO and CTF (Figure 7(a)). However, with intermittent light (CTA), abrupt expansion occurred during the heating period and successive contraction over the cooling intervals. In response to moisture variations, more

expansion occurred with increasing humidity and more contraction with decreasing humidity. In contrast, the colonized rock surface remained stable when the lamp was off (CHF) (Figure 7(b)). Under varying temperature, a thermal contraction was also observed on the non-colinized surface (Figure 7(c)); while under varying humidity, the non-colonized rock surface was relatively stable except for the continuous expansion under NHO (Figure 7(d)). In general, contraction and expansion tended to occur concurrently across the rock surface, expect when stability was the dominant surface movement trend (Table V).

As the common concurrence of expansion and contraction across the surface, volumetric changes of the surface of the two blocks were used to demonstrate the magnitude of surface movements, to represent the overall 2-hourly surface movement trend throughout each treatment (Figure 8). The values were calculated with relative height data and therefore determined as 0 cm^3 when all probe readings were of 0 mm. Changes ranging from 0.2 to 0.3 cm^3 (equivalent to overall elevation changes ranging from 0.05 to 0.08 mm across the surface) were common on the colonized site under varying air temperature (Figure 8(a)). Here, the surface tended to contract with increasing temperature, reach the lowest volumetric changes at the hottest hour and expand during the cooling period. Under varying humidity, the highest volumetric changes of the colonized rock surface occurred when humidity was increasing, while the lowest changes at the driest hours (CHF) (Figure 8(b)). Compared with other light conditions, the colonized rock surface with intermitten light underwent more oscillations in volumetric changes (CTA and CHA). A pattern of thermal contraction was observed on the non-colonized rock surface in that the lowest volumetric change occurred when temperature reached its maximum (Figure 8(c)). No evident

change patterns were observed with varying humidity, except for a continuous expansion under NHO (Figure 8(d)). Although undergoing fluctuations throughout the running, in general, volumetric changes on the two blocks were reversible that the blocks tended to recover to their initial volume at the end of the 14-hour simulation.

The influence of environmental factors

Although only one significant ($P < 0.05$) linear relationship was demonstrated (NTF) among 12 treatments, the x-y intercept of regression equation could suggest the general trend of surface movements under the influence of varying environmental factors, with its correlation coefficient ranging from moderate to high (Figure 9) (Table VI). Both rock surfaces appeared to expand with decreasing temperature and contract with increasing temperature. This movement trend on the colonized rock surface was influenced by light condition with moderate and strong relationships (R^2 = 0.26 and 0.45) only occurring when the lamp was on (CTO in Figure 9(a) and (b)). In comparison, moderate and strong relationships (R^2 ranging from 0.17 to 0.88) were shown on the non-colonized rock surface regardless of the light condition (Figure 9(d) and (e)). Relationships between rock surface changes and varying humidity ranged from low to non-existent for two types of block, with an exception of moderate relationship on the colonized rock surface under CHO (R^2 = 0.19) (Figure 9(c) and (f)).

To further assess the influence of light on rock surface changes, the one-way analysis of variance (ANOVA) and Tukey's highly significant difference test (HSD) were used to

examine differences in the mean magnitude of surface movements between three treatments which were only of differing lamp conditions, and determine their grouping information (Hemmingsen *et al.*, 2007) (Table VII). The null hypotheses that the lamp condition did not influence the mean magnitude of rock surface changes were rejected in all cases. At least two out of three comparisons within each simulation were significantly different.

The overall rock surface change

To investigate the linkage between the short- and long-term surface change, the overall rock surface change was calculated by comparing the first (2 hours) and last (14 hours) measurements of each when the microclimate was at the same condition (Table VIII). Although more than half of changes were measurable under 9 treatments, the range of median (-0.032 to +0.033 mm) was of lower magnitude compared with 2-hourly surface changes. The *t*-test was used to assess if there were significant surface changes occurring over the 12-hour experiment, with the threshold of measurable surface movement ±0.010 mm to determine the overall surface movement trend. If the upper bound of the 95% confidential interval is less than -0.010 mm, the rock surface was of significant overall falling trend. If the lower bound of the 95% confidential interval is greater than +0.010 mm, the rock surface was of significant overall rising trend. Otherwise the rock surface was regarded as stable over the entire experiment. Under half of the treatments (6), the rock surface tended to remain stable; while significant falling trend was observed under 5

treatments. Only one overall expansion was demonstrated on the non-colonized surface in response to the varying humidity (NHO).

Discussion

In this laboratory study, on the colonized rock surface, the maximum movement of a single point ranged from -0.281 to +0.238 mm (-0.281 to +0.235 mm under varying temperature and -0.187 to +0.238 mm under varying humidity), 34% higher than the range (-0.126 to +0.261 mm) recorded by Gómez-Pujol *et al.* (2007) at Marengo and 21% lower than the range (-0.287 to +0.371 mm) recorded by Yuan *et al.* (2018) at the same site. The median value of surface movements varied from -0.072 to +0.068 mm (-0.072 to +0.053 mm under varying temperature and -0.040 to +0.068 mm under varying humidity), comparable with the range of -0.050 to +0.041 mm found on supratidal sandstone at Marengo (Yuan *et al.* 2018). Based on the similar magnitude of microtopographic fluctuations measured in the laboratory compared to previous studies at Marengo, we infer that the processes are comparable between the laboratory and the field.

Under the same environmental condition, the magnitude and pattern of surface movements were significantly different between the colonized and the non-colonized rock surfaces, indicating the primary role of lithobiontic biofilms in driving microtopographic fluctuations of supratidal sandstone. Particularly under varying humidity, on average, the magnitude of surface movements on the colonized block was much higher by 121 - 154% (CHO/NHO and CHA/NHA) (Table IV). The colonized rock surface tended to expand with increasing humidity and contract with decreasing humidity (CHO and CHA), which is in

accord with the previous field studies at Marengo (Gómez-Pujol *et al.*, 2007; Yuan *et al.*, 2018). According to the SEM examination on rock specimen collected from Marengo, the diameter of hyphae in biofilms is around 16 μm and fluctuating humidity can cause increases or decreases of 12 μm, resulting in the range of hyphae widths between 0.010 and 0.022 mm (Gómez-Pujol *et al.*, 2007). These values are high enough to cause the magnification of 2-hourly surface changes measured on the colonized block (Table IV). With the highly hydrophilic substances in lithobiontic microorganism communities (such as green algal lichens), water vapour can be absorbed and equilibrated with air from extremely low values to supersaturation within hours or minutes (Larson, 1987; Snethlage and Wendler, 1997). The magnitude of surface movements in the laboratory equates to the microtopographic fluctuations induced by the biofilm mechanism, confirming the inference of Gómez-Pujol *et al.* (2007). In comparison, no obvious surface change pattern was demonstrated on the non-colonized block with changing humidity, except for a continuous expansion occurring under NHO treatment. Crystalline and osmotic swelling of clay minerals as well as disjoining pressure is a likely mechanism for this expansion in sandstone (Butt *et al.*, 2006; Ruedrich *et al.*, 2011), and rocks which are clay-poor or-free but rich in micropores, such as granite and marble (Weiss, 1992; Schult and Shi, 1997).

Significant surface movements were observed on the colonized rock surface under varying temperature when humidity was constant. Air temperature plays an important role in controlling water content of hyphae and other biofilm elements by supplying heat to sustain evaporation (Monteith, 1965; Larson, 1987). Lithobiontic biofilms lose water with increasing temperature and reach the minimum water content at the hottest time of the day

(Lange *et al.*, 1990; Lange *et al.*, 2006). Consequently, the photosynthetic activity is limited by desiccation (Tretiach and Geletti, 1997); and lithobiontic biofilms only recover from dehydration and absorb water when temperature declines to the suitable range for their physiological activity.

However, thermal contraction of similar order of magnitude (ranging from -0.308 to +0.297 mm) also occurred on the non-colonized rock surface. This pattern is opposite to the previous studies that show rock surfaces expand with increasing temperature and contract with deceasing temperature (Hall and Hall, 1991; Bland and Rolls, 1998). It is possible in a highly humid environment, increasing temperatures can cause the loss of adsorbed water in clay minerals and subsequently reduce the related moisture expansion. The lowering of adsorbed water in micropores also decreases the disjoining pressure, resulting in the contraction of rock (Ruedrich *et al.*, 2011). Except for the loss of free or adsorbed water in rocks, high temperatures reduce the water from other sources, such as the interlayer water from very close mineral surfaces and chemically combined water from hydration reaction (Halsey *et al.*, 1998). Thermal contraction related to decreasing moisture content has been confirmed by recent research, such as shrinking of rocks with clay minerals (Weiss *et al.*, 2004) or zeolitic cements (Di Benedetto *et al.*, 2015). Although the mechanism of rock moisture expansion was not the focus of this study, with a difference of 21°C in temperature, thermal contractions of 0.14 - 0.35 cm^3 were measured on the non-colonized rock surface (Figure 8(c)).

From the linear regression analysis, significant correlationships between surface movements and variations of air temperature or relative humidity identified in the field

(Yuan et al., 2018) were barely examined in the laboratory (Table VI). It is probably partially caused by the small amount of data (6 points for each treatment) used for the analysis, or isolating the influence of individual environmental factor during the simulation. The less significant relationships imply the complexity of mechanisms operating on hourly microtopographic fluctuations and responses of rock surfaces to microclimatic variations.

The role of light in rock surface changes was identified on the colonized block, particularly from its responses to moisture variations. Since the lack of capacity for photosynthetic energy conservation, poikilohydry (i.e. the water status of plants is completely dependent on their environment) is commonly exhibited in lithobiontic microorganism communities of which the physiology is under the close control of light (Lange *et al.*, 1994; Heber and Lüttge, 2011). Strong solar radiation can drive photosynthesis and promote water loss from thalli (Lange *et al.*, 1990). Dry hyphae tends to stay inactive with high light intensity; when the light intensity decreases, desiccation ceases and hydration can quickly occur with sufficient ambient humidity (Heber and Lüttge, 2011). Under CHO with the lamp on, the initial overall expansion likely indicates a near instantaneous rehydration of hyphae with increasing humidity, while the continuous strong light may depress the net rate of photosynthesis afterwards. Thus hyphae or biofilms dehydrated gradually over the remaining observation. Induced by the photosensitivity of lithobiontic biofilms, the surface change pattern in response to moisture variations was interrupted by intermittent light (CHA). Because biofilms could lose water under strong light and rehydrate in the dark to equilibrate with the ambient humidity. This interrupted pattern was also found with changing temperature (CTA). In the simulated night environment, the physiological activity

of biofilms was inhibited without light. As a result, the colonized rock surface could maintain relatively stable under fluctuating humidity (CHF). On the non-colonized block, thermal contractions of significantly different magnitudes were shown between three lamp conditions (Figure 8(c)). This could be related to subsurface rock temperature since differences in surface temperature were < 1°C (Figure 6(c)). Due to the difficulty in detecting rock temperature at depths in the field environment, rock surface temperature has been a complementary information source and the temperature gradient between rock surface and subsurface was not fully discussed in the previous short-term microtopographic change field studies (Gómez-Pujol *et al.*, 2007; Mayaud *et al.*, 2014; Yuan *et al.*, 2018). Given that thermal gradient causes the stressing of rock and ultimately rock decay through thermal fatigue effects and interacts with the colonized organism on rock surfaces (Warke *et al*., 1996; Warke and Smith, 1998; Coombes and Naylor, 2012), this omission needs to be justified in the future field and laboratory study.

Despite the dynamic surface movement and the complex operating mechanisms, when the microclimatic conditions at the beginning and end of simulation were equivalent, there appeared to be no net volumetric change occurring on the block over the course of test (Figure 8) (Table VIII). This was also found from the 30-hour field observation at Marengo (Yuan *et al.*, 2018). It suggests the 2-hourly rock surface changes induced by fluctuating microclimate are reversible, react promptly to the changing environmental factors without lag effects and causes no loss of material on the block. The impact of short-term surface change on rock decay cannot be observed unless its cumulative effect can lead to rock failure (e.g. granular disintegration and spalling), as implied by the overall contraction over

12-hour observations (Table VIII) (Figure 10). In this hourly-scale study, the lithobiontic biofilms caused higher microtopographic fluctuations and more repeated expansion and contraction on the colonized block, which could facilitate the detachment of grains and granular-scale erosion on the rock surface by generating greater stresses and fatigue in rock surfaces, and consequently contribute to rock decay and accelerating the rate of breakdown of supratidal rock (Sunamura, 1992; Stephenson *et al.*, 2004). Over longer temporal scales, due to the enhancement of moisture retention on rock surfaces, the colonized biofilms may play a bioprotective role in rock decay by buffering thermal extremes and decreasing the efficiency of thermal fatigue in rock bodies (Coombes and Naylor, 2012). To fully understand the influence of lithobiontic biofilm on coastal rock decay and the linkage between short-term surface dynamics and long-term surface change pattern, future observations on the pattern and magnitude of rock surface change across multi-timescales are needed in the laboratory experiments.

Conclusions

Using microclimate simulation experiments, hourly rock surface changes on a sandstone block with colonized lithobiontic biofilms were observed to be induced by univariate environmental factors, including air temperature and humidity. Changes of 7°C in air temperature or 14% in relative humidity were sufficient enough to cause surface movements ranging from -0.281 to +0.235 mm and -0.187 to +0.238 mm respectively.

Compared with observations on the non-colonized sandstone block, the magnitude of surface movement on the colonized block was higher by 12 - 120% in response to varying

tempeature and more significantly (121 - 154%) to varying humidity, confirming the lithobiontic biofilm to be the primary mechanism of hourly surface changes on the supratidal sandstone at Marengo, Australia. Controlled by the water status of biofilms, the colonized rock surface tended to expand with increasing humidity and contract with decreasing humidity. An inverse pattern was observed in response to thermal variations. These surface movement patterns were interrupted under intermitten light, probably by influening the physiology of lithobiontic biofilms. However, thermal contraction ranging from -0.308 to +0.297 mm also occurred on the non-colonized block, indicating the lithobiontic biofilm is not the primary driver in this dynamic process.

Despite the hourly rock surface dynamics in the mechanism of colonized biofilms does not cause the loss of material directly, the intensified magnitude and more cycles of expansion and contraction could accelerate the detachment of grains and granular disintegration on rock surfaces, contributing to rock decay. We have then demostrated the potential role of lithobiontic biofilms in supratidal sandstone rock decay and the linkage between the short- and long-term rock surface change.

Acknowledgements

This work was partly funded by The Australian Research Council (Grant #LP130100204). Thomas Savige is thanked for sample collection in the field. Darren Hocking is thanked for assistance in the laboratory testing.

References

BoM, 2016. *Long-term temperature record*. Bureau of Meteorology: Canberra.

Bland W, Rolls D. 1998. *Weathering: an introduction to the scientific principles.* Arnold: London.

Butt HJ, Graf K, Kappl M. 2006. *Physics and chemistry of interfaces*. John Wiley and Sons: Chichester.

Carter NEA, Viles HA. 2004. Lichen hotspots: raised rock temperatures beneath Verrucaria nigrescens on limestone. *Geomorphology* **62:** 1-16.

Cockell CS, Hecht L, Landenmark H, Payler SJ, Snape M. 2018. Rapid colonization of artificial endolithic uninhabited habitats. *International Journal of Astrobiology* **17:**386-401.

Coombes MA. 2011. Rock warming and drying under simulated intertidal conditions, part I: experimental procedures and comparisons with field data. *Earth Surface Processes and Landforms* **36:** 2114–2121.

Coombes MA. 2014. The rock coast of the British Isles: weathering and biogenic processes. In *Rock Coast Geomorphology: A Global Synthesis*, Kennedy DA, Stephenson WJ, Naylor LA (eds). Geological Society: London; 57-76.

Coombes MA, Naylor LA. 2012. Rock warming and drying under simulated intertidal conditions, part II: weathering and biological influences on evaporative cooling and near-surface micro-climatic conditions as an example of biogeomorphic ecosystem engineering. *Earth Surface Processes and Landforms* **37:** 100–118.

Di Benedetto C, Cappelletti P, Favaro M, Graziano S, Langella A, Calcaterra D, Colella A. 2015. Porosity as key factor in the durability of two historical building stones: Neapolitan Yellow Tuff and Vicenza Stone. *Engineering Geology* **193:** 310-319.

Foote Y, Plessis E, Robinson D, Hanaff A, Costa S. 2006. Rates and patterns of downwearing of chalk shore platforms of the Channel Coasts: Comparisons between France and England. *Zeitschrift fur Geomorphologie Supplementband* **144:** 93-115.

Gómez-Pujol L, 2014. De la costa al laboratorio: respuesta de superficies carbonatadas colonizadas y libres a oscilaciones ambientales. In *Avances de la Geomorfología en España 2012-2014*, Schnabel S, Gómez A (eds). Universidad de Extremadura: Cáceres; 576-579.

Gómez-Pujol L, Stephenson WJ, Fornós JJ. 2007. Two-hourly surface change on supra-tidal rock (Marengo, Victoria, Australia). *Earth Surface Processes and Landforms* **32:** 1-12.

Gowell MR, Coombes MA, Viles HA. 2015. Rock-protecting seaweed? Experimental evidence of bioprotection in the intertidal zone. *Earth Surface Processes and Landforms* **40:** 1364-1370.

Hall K, Hall A. 1991. Thermal gradients and rock weathering at low temperatures: some simulation data. *Permafrost and Periglacial Processes* **2:** 103-112.

Hall K, Thorn CE. 2014. Thermal fatigue and thermal shock in bedrock: An attempt to unravel the geomorphic processes and products. *Geomorphology* **206**, 1-13.

Halsey D, Mitchell D, Dews S. 1998. Influence of climatically induced cycles in physical weathering. *Quarterly Journal of Engineering Geology and Hydrogeology* **31:** 359-367.

Heber U, Lüttge U. 2011. Lichens and bryophytes: light stress and photoinhibition in desiccation/rehydration cycles–mechanisms of photoprotection. In *Plant Desiccation Tolerance*, Lüttge U, Beck E, Barthels D (eds). Springer: Berlin; 121-137.

Hemmingsen SA, Eikaas HS, Hemmingsen MA. 2007. The influence of seasonal and local weather conditions on rock surface changes on the shore platform at Kaikōura Peninsula, South Island, New Zealand. *Geomorphology* **87:** 239-249.

High CJ, Hanna FK. 1970. A Method for the Direct Measurement of Erosion on Rock Surfaces. *British Geomorphological Research Group Technical Bulletin* **5:** 1-25.

Kirk R. 1977. Rates and forms of erosion on intertidal platforms at Kaikoura Peninsula, South Island, New Zealand. *New Zealand Journal of Geology and Geophysics* **20:** 571-613.

Lange OL, Meyer A, Zellner H, Ullmann I, Wessels D. 1990. Eight days in the life of a desert lichen: water relations and photosynthesis of Teloschistes capensis in the coastal fog zone of the Namib Desert. *Madoqua* **17:** 17-30.

Lange OL, Meyer A, Zellner H. Heber, U., 1994. Photosynthesis and Water Relations of Lichen Soil Crusts: Field Measurements in the Coastal Fog Zone of the Namib Desert. *Functional Ecology* **8:** 253-264.

Lange OL, Tga G, Melzer B, Meyer A, Zellner H. 2006. Water relations and CO_2 exchange of the terrestrial lichen Teloschistes capensis in the Namib fog desert: Measurements during two seasons in the field and under controlled conditions. *Flora* **201:** 268-280.

Larson DW. 1987. The absorption and release of water by lichens. *In Progress and Problems in Lichenology in the Eighties*, Peveling E (eds). Bibliothca lichenologica 25 J. Cramer: Berlin; 351–360.

Leznicka S, Strzelczyk A, Wandrychowska D. 1988. Removing of fungal stains from stone-works, In *IV International Congress on Deterioration and Conservation of Stone*. Nicolaus Copernicus University: Torun; 102–110.

Matthews JA. 1981. *Quantitative and statistical approaches to geography: a practical manual*. Pergamon press: Oxford.

Mayaud JR, Viles HA, Coombes MA. 2014. Exploring the influence of biofilm on short-term expansion and contraction of supratidal rock: an example from the Mediterranean. *Earth Surface Processes and Landforms* **39:** 1404-1412.

McKenna TE, Sharp Jr JM, Lynch FL. 1996. Thermal conductivity of Wilcox and Frio sandstones in south Texas (Gulf of Mexico Basin). *AAPG bulletin*, **80:** 1203-1215.

Monteith JL. 1965. Evaporation and environment. *Symp. Soc. Exp. Biol* **19:** 205-234.

Mottershead D. 1989. Rates and patterns of bedrock denudation by coastal salt spray weathering: A seven-year record. *Earth Surface Processes and Landforms* **14:** 383-398.

National Physical Laboratory (NPL), 2010. Kaye and Laby Table of Physical and Chemical Components. http://www.kayelaby.npl.co.uk/general_physics/2_3/2_3_5.html.

Naylor LA, Stephenson WJ. 2010. On the role of discontinuities in mediating shore platform erosion. *Geomorphology* **114:** 89-100.

Porter NJ, Trenhaile AS, Prestanski KJ, Kanyaya JI. 2010. Shore platform downwearing in eastern Canada: micro-tidal Gaspe, Quebec. *Geomorphology* **116:** 77-86.

Ruedrich J, Bartelsen T, Dohrmann R, Siegesmund S. 2011. Moisture expansion as a deterioration factor for sandstone used in buildings. *Environmental Earth Sciences* **63:** 1545-1564.

Spencer T. 1981. Micro-topographic change on calcarenites, grand Cayman Island, West Indies. *Earth Surface Processes and Landforms* **6:** 85-94.

Schult A, Shi G. 1997. Hydration swelling of crystalline rocks. *Geophysical Journal International* **131:** 179-186.

Smith B, Warke P, McGreevy J, Kane H. 2005. Salt-weathering simulations under hot desert conditions: agents of enlightenment or perpetuators of preconceptions? *Geomorphology* **67:** 211-227.

Snethlage R, Wendler E. 1997. Moisture cycles and sandstone degradation. In *Saving our architectural heritage: The conservation of historic stone structures*, Baer NS, Snethlage R (eds). Elsevier: Chichester; 7-24.

Stephenson WJ, Finlayson BL. 2009. Measuring erosion with the micro-erosion meter—contributions to understanding landform evolution. *Earth-Science Reviews* **95:** 53-62.

Stephenson WJ, Kirk RM. 1996. Measuring erosion rates using the micro-erosion meter: 20 years of data from shore platforms, Kaikōura Peninsula, South Island, New Zealand. *Marine Geology* **131:** 209-218.

Stephenson WJ, Kirk RM. 2001. Surface swelling of coastal bedrock on inter-tidal shore platforms, Kaikōura Peninsula, South Island, New Zealand. *Geomorphology* **41:** 5-21.

Stephenson WJ, Taylor AJ, Hemmingsen MA, Tsujimoto H, Kirk RM. 2004. Short-term microscale topographic changes of coastal bedrock on shore platforms. *Earth Surface Processes and Landforms* **29:** 1663-1673.

Sunamura, T. 1992. *Geomorphology of rocky coasts*. John Wiley and Sons: Chichester.

Swantesson JOH, Gómez-Pujol L, Cruslock EM, Fornós JJ, Balaguer P. 2006. Processes and patterns of erosion and downwearing on micro-tidal rock coasts in Sweden and the western Mediterranean. In *European Shore Platform Dynamics*, Robinson DA, Lageat Y (eds). Zeitschrift für Geomorphologie: Supplementbänd; 137-160.

Taylor, AJ. 2003. *Change and processes of change on shore platforms*. PhD thesis, University of Canterbury: Christchurch.

Trenhaile AS. 2006. Tidal wetting and drying on shore platforms: an experimental study of surface expansion and contraction. *Geomorphology* **76:** 316-331.

Trenhaile AS, Porter NJ. 2018. Shore platform downwearing in eastern Canada; A 9–14 year micro-erosion meter record. *Geomorphology* **311:** 90-102.

Tretiach M, Geletti A. 1997. CO_2 exchange of the endolithic lichen Verrucaria baldensis from karst habitats in northern Italy. *Oecologia* **111:** 515-522.

Trudgill S, High CJ, Hanna FK. 1981. Improvements to the Micro-erosion meter. *British Geomorphological Research Group Technical Bulletin* **29:** 3-17.

Warke P, Smith, B. 1998. Effects of direct and indirect heating on the validity of rock weathering simulation studies and durability tests. *Geomorphology* **22:** 347-357.

Warke P, Smith B, Magee R. 1996. Thermal response characteristics of stone: implications for weathering of soiled surfaces in urban environments.*Earth Surface Processes and Landform*s **21:** 295–306.

Weiss G. 1992. Die Eis-und Salzkristallisation im Porenraum von Sandsteinen und ihre Auswirkungen auf das Gefüge unter besonderer Berücksichtigung gesteinsspezifischer Parameter. *Münchner Geowissenschaftliche Abhandlungen*, Reihe Band: 62.

Weiss T, Siegesmund S, Kirchner Dt, Sippel J. 2004. Insolation weathering and hygric dilatation: two competitive factors in stone degradation. *Environmental Geology* **46**: 402-413.

Yuan R, Kennedy DM, Stephenson WJ. 2018. Hourly to daily-scale microtopographic fluctuations of supratidal sandstone. *Earth Surface Processes and Landforms*. DOI: 10.1002/esp.4476

Tables

Table I. Conditions and identification (ID) code for each of the 12 different treatments

No.	Surface type	Variable	Lamp condition	ID
1	Colonized (C)	Temperature (T)	On (O)	CTO
2	Colonized (C)	Temperature (T)	On and off (A)	CTA
3	Colonized (C)	Temperature (T)	Off (F)	CTF
4	Colonized (C)	Humidity (H)	On (O)	CHO
5	Colonized (C)	Humidity (H)	On and off (A)	CHA
6	Colonized (C)	Humidity (H)	Off (F)	CHF
7	Non-colonized (N)	Temperature (T)	On (O)	NTO
8	Non-colonized (N)	Temperature (T)	On and off (A)	NTA
9	Non-colonized (N)	Temperature (T)	Off (F)	NTF
10	Non-colonized (N)	Humidity (H)	On (O)	NHO
11	Non-colonized (N)	Humidity (H)	On and off (A)	NHA
12	Non-colonized (N)	Humidity (H)	Off (F)	NHF

Table II. The magnitude of microtopographic fluctuations (mm) under 12 treatments

Treatment	Percentage of measurable change (%)	Maximum movement range	Median value range	Mean	SD
CTO	57.3	-0.263 to 0.216	-0.049 to 0.022	-0.003	0.047
CTA	74.4	-0.217 to 0.235	-0.072 to 0.053	0.001	0.064
CTF	45.0	-0.281 to 0.142	-0.068 to 0.046	-0.001	0.051
CHO	62.2	-0.165 to 0.238	-0.026 to 0.068	0.002	0.051
CHA	56.8	-0.187 to 0.138	-0.040 to 0.027	-0.005	0.046
CHF	39.4	-0.090 to 0.103	-0.007 to 0.002	-0.003	0.022
BTO	57.3	-0.308 to 0.297	-0.064 to 0.047	-0.005	0.060
BTA	79.7	-0.232 to 0.260	-0.036 to 0.061	-0.004	0.056
BTF	43.4	-0.073 to 0.094	-0.015 to 0.015	0.000	0.020
BHO	53.6	-0.053 to 0.084	-0.012 to 0.024	0.006	0.018
BHA	33.7	-0.088 to 0.099	-0.009 to 0.017	0.002	0.019
BHF	31.5	-0.095 to 0.088	-0.006 to 0.015	0.001	0.020

Table III. The *t*-test statistic values and significant values for each pair of comparison. *P* values in bold refer to significant difference

Hour	2 to 4		4 to 6		6 to 8		8 to 10		10 to 12		12 to 14	
	t	*P*	*t*	*P*	*t*	*P*	*t*	*P*	*t*	*P*	*t*	*P*

CTO/NTO	4.31	**< 0.001**	0.54	0.6	0.61	0.5	-2.78	**0.006**	3.57	**0.001**	0.47	0.6
CTA/NTA	-7.67	**< 0.001**	9.08	**< 0.001**	2.29	**0.02**	0.42	0.7	-8.48	**< 0.001**	8.81	**< 0.001**
CTF/NTF	0.68	0.5	-8.37	**< 0.001**	10.46	**< 0.001**	6.72	**< 0.001**	-7.31	**< 0.001**	-10.24	**< 0.001**
CHO/NHO	9.35	**< 0.001**	-5.9	**< 0.001**	-2.87	**0.005**	-13.76	**< 0.001**	-9.43	**< 0.001**	4.19	**< 0.001**
CHA/NHA	-1.31	0.19	5.48	**< 0.001**	4.09	**< 0.001**	-5.57	**< 0.001**	1.03	0.3	-6.86	**< 0.001**
CHF/NHF	-3.87	**< 0.001**	-2.06	**0.04**	-2.89	**0.005**	5	**< 0.001**	4.05	**< 0.001**	-6.03	**< 0.001**

Table IV. Mean values of the absolute value of 2-hourly rock surface change under each treatment and *t*-tests of difference in magnitude between two types of blocks. *Magnification factor = (colonized – non-colonized) / non-colinized × 100%*. Positive values indicate higher magnitude of surface change occurring on the colonized block and otherwise occurring on the non-colonized block. *P* values in bold refer to significant difference

Variable	Lamp condition	Comparison	Colonized (mm)	Non-colonized (mm)	Magnification factor (%)	*t*	*P*
Temperature	On	CTO/NTO	0.029	0.035	-18	-2.36	**0.02**
	On and off	CTA/NTA	0.046	0.041	12	2.02	**0.04**
	Off	CTF/NTF	0.029	0.013	120	8.58	**< 0.001**
Humidity	On	CHO/NHO	0.032	0.015	121	10.03	**< 0.001**
	On and off	CHA/NHA	0.030	0.012	154	11.44	**< 0.001**
	Off	CHF/NHF	0.014	0.012	14	1.65	0.1

Table V. Percentages of rising, falling and stable points occurring in each 2-hour interval (%)

Treatment	Trend	2 to 4	4 to 6	6 to 8	8 to 10	10 to 12	12 to 14
	Rising	16.1	10.8	17.2	59.1	41.9	4.3
CTO	Falling	45.2	28.0	72.0	17.2	19.4	12.9
	Stable	38.7	61.3	10.8	23.7	38.7	82.8
	Rising	14.0	76.3	26.9	11.8	5.4	72.0
CTA	Falling	79.6	9.7	44.1	51.6	36.6	18.3
	Stable	6.5	14.0	29.0	36.6	58.1	9.7
	Rising	5.4	15.1	72.0	57.0	1.1	0.0
CTF	Falling	11.8	74.2	16.1	15.1	2.2	0.0
	Stable	82.8	10.8	11.8	28.0	96.8	100.0
	Rising	72.0	19.4	32.3	2.2	17.2	25.8
CHO	Falling	22.6	61.3	6.5	44.1	65.6	4.3
	Stable	5.4	19.4	61.3	53.8	17.2	69.9
	Rising	22.6	40.9	1.1	16.1	64.5	18.3
CHA	Falling	4.3	7.5	3.2	72.0	22.6	67.7
	Stable	73.1	51.6	95.7	11.8	12.9	14.0
	Rising	25.8	2.2	6.5	28.0	36.6	17.2
CHF	Falling	7.5	9.7	44.1	8.6	2.2	48.4
	Stable	66.7	88.2	49.5	63.4	61.3	34.4
	Rising	2.2	10.8	21.5	64.5	28.0	4.3
NTO	Falling	58.1	39.8	71.0	24.7	4.3	15.1
	Stable	39.8	49.5	7.5	10.8	67.7	80.6
	Rising	4.3	34.4	23.7	32.3	75.3	20.4
NTA	Falling	65.6	28.0	63.4	49.5	16.1	65.6
	Stable	30.1	37.6	12.9	18.3	8.6	14.0
	Rising	2.2	0.0	12.9	1.1	59.1	58.1
NTF	Falling	35.5	14.0	61.3	7.5	7.5	1.1
	Stable	62.4	86.0	25.8	91.4	33.3	40.9
	Rising	1.1	39.8	47.3	78.5	47.3	9.7
NHO	Falling	53.8	6.5	2.2	5.4	5.4	24.7
	Stable	45.2	53.8	50.5	16.1	47.3	65.6
	Rising	33.3	4.3	0.0	15.1	66.7	3.2
NHA	Falling	6.5	7.5	17.2	44.1	3.2	1.1
	Stable	60.2	88.2	82.8	40.9	30.1	95.7
	Rising	54.8	1.1	0.0	1.1	36.6	15.1
NHF	Falling	15.1	2.2	12.9	4.3	43.0	3.2
	Stable	30.1	96.8	87.1	94.6	20.4	81.7

Table VI. The linear trend between each environmental factor and median values of relative height difference over 2-hour intervals for 12 different treatments. *P* values in bold refer to significant linear relationship

Figure	Treatment	Regression equation	R^2	*P*
7(a)	CTO	MD = -0.0021 AT - 0.0061	0.45	0.15
	CTA	MD = -0.0015 AT + 0.0027	0.06	0.6
	CTF	MD = -0.0011 AT - 0.0005	0.05	0.7
7(b)	CTO	MD = -0.0023 RT - 0.0053	0.26	0.3
	CTA	MD = -0.0012 RT + 0.0031	0.02	0.8
	CTF	MD = -0.0010 RT + 0.0002	0.02	0.8
7(c)	CHO	MD = 0.0010 H + 0.0035	0.19	0.4
	CHA	MD = 0.0007 H - 0.0073	0.15	0.4
	CHF	MD = -0.0001 H - 0.0018	0.06	0.6
7(d)	NTO	MD = -0.0032 AT - 0.0055	0.46	0.14
	NTA	MD = -0.0018 AT - 0.0026	0.17	0.4
	NTF	MD = -0.0012 AT + 0.0002	0.59	0.07
7(e)	NTO	MD = -0.0039 RT - 0.0036	0.38	0.2
	NTA	MD = -0.0028 RT - 0.0012	0.19	0.4
	NTF	MD = -0.0020 RT + 0.0015	0.88	**0.006**
7(f)	NHO	MD = -0.0003 H + 0.0062	0.16	0.4
	NHA	MD = -0.0001 H + 0.0017	0.04	0.7
	NHF	MD = 0.0001 H + 0.0015	0.01	0.8

Table VII. Results of the ANOVA and Tukey's HSD test (*P* values in bold refer to significant difference. O: lamp on, A: lamp on and off, F: lamp off)

Simulation	Treatment	*F*	*P*	Grouping
Colonized & Varying temperature	CTO	31.96	**< 0.001**	A
	CTA			B
	CTF			A
Colonized & Varying humidity	CHO	55.93	**< 0.001**	A
	CHA			A
	CHF			B
Non-colonized & Varying temperature	NTO	87.18	**< 0.001**	A
	NTA			B
	NTF			C
Non-colonized & Varying humidity	NHO	5.37	**0.005**	A
	NHA			B
	NHF			B

Table VIII. The magnitude (mm) and overall trend of microtopographic fluctuations under 12 treatments (from 2 to 14 hours)

Treatment	Percentage of measurable change (%)	Median	Mean	SD	95% CI	Overall trend
CTO	71.0	-0.014	-0.017	0.026	(-0.022, -0.012)	Falling
CTA	46.2	0.002	0.006	0.033	(-0.001, 0.012)	Stable
CTF	21.5	-0.004	-0.007	0.008	(-0.008, -0.005)	Stable
CHO	55.9	0.010	0.013	0.028	(0.008, 0.019)	Stable
CHA	84.9	-0.032	-0.030	0.040	(-0.039, -0.022)	Falling
CHF	58.1	-0.010	-0.016	0.026	(-0.021, -0.011)	Falling
NTO	93.5	-0.026	-0.030	0.018	(-0.034, -0.026)	Falling
NTA	84.9	-0.022	-0.022	0.031	(-0.028, -0.015)	Falling
NTF	31.2	-0.003	-0.002	0.014	(-0.005, 0.001)	Stable
NHO	84.9	0.033	0.035	0.034	(0.028, 0.042)	Rising
NHA	53.8	0.010	0.014	0.021	(0.009, 0.019)	Stable
NHF	52.7	0.008	0.007	0.018	(0.003, 0.011)	Stable

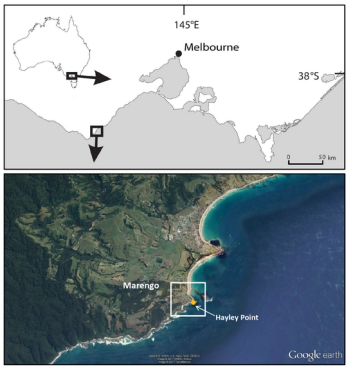

ESP_4581_Figure 1.tif

ESP_4581_Figure 2.tif

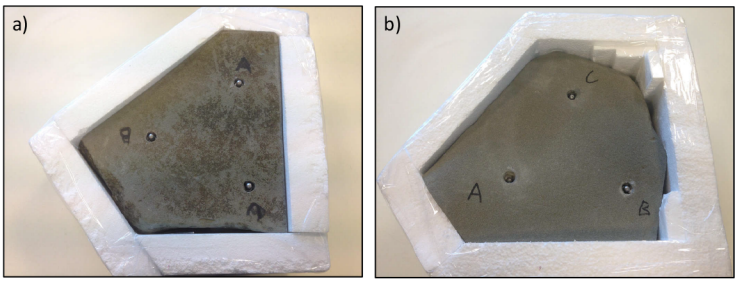

ESP_4581_Figure 3.tif

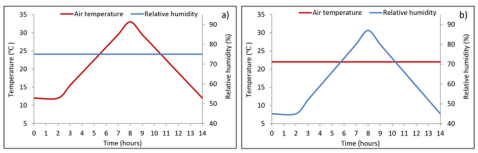

ESP_4581_Figure 4.tif

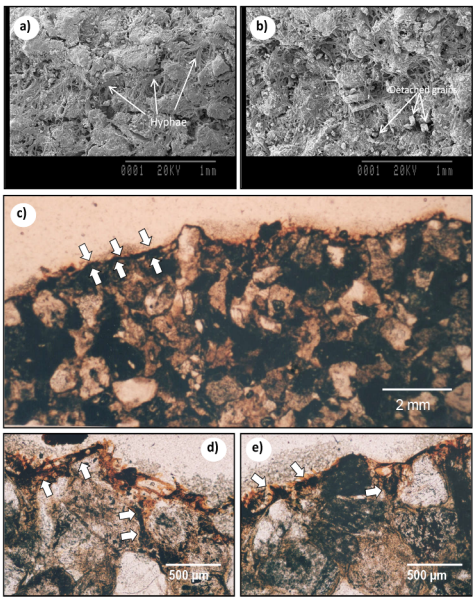

ESP_4581_Figure 5.tif

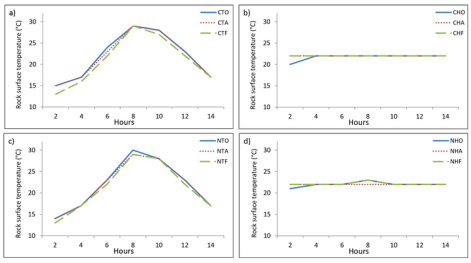

ESP_4581_Figure 6.tif

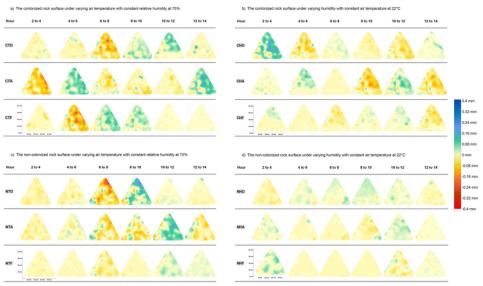

ESP_4581_Figure 7.tif

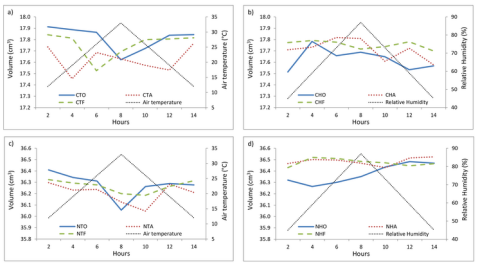

ESP_4581_Figure 8.tif

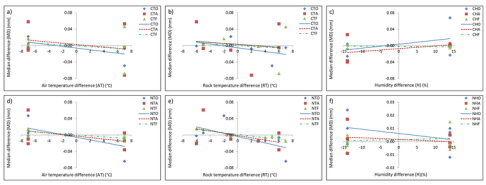

ESP_4581_Figure 9.tif

ESP_4581_Figure 10.tif

Figure 1. Location of the study site at Marengo, Victoria, Australia.

Figure 2. The shore platform and cliff at Hayley Point, Marengo, where the test sandstone was collected.

Figure 3. Two studied sandstone blocks: (a) the colonized rock surface and (b) the non-colonized rock surface. The distance between two bolts is 160 mm.

Figure 4. Profiles designed to study the impact of different environmental parameters: (a) the simulation for temperature with a constant relative humidity of 75% and (b) the simulation for humidity with a constant air temperature of 22°C.

Figure 5. Scanning electron microscope (SEM) images of surfaces of rock samples collected from Marengo: (a, b) general views of intense biofilm colonization on the rock surface; (c, d and e) thin-sections of rock surface colonized by lithobiontic biofilms. Arrows indicate biofilms colonizing on the surface and hyphae penetrating deep into the crevices between grains.

Figure 6. Variations of rock surface temperature under 12 treatments (Upper panels for the colonized rock surface, lower panels for the non-colonized rock surface. O: lamp on, A: lamp on and off, F: lamp off).

Figure 7. Contour graphs for 2-hourly microtopographic changes under 12 treatments. Each graph shows the magnitude of microtopographic fluctuations occurring over 2-hour interval. Movements greater than 0.01 mm (blue and green) stand for expansion, less than -0.01 mm (yellow and red) for contraction and within ± 0.01 mm (white and faint yellow) for stability (Upper panels for the colonized rock surface, lower panels for the non-colonized rock surface. O: lamp on, A: lamp on and off, F: lamp off).

Figure 8. Volumetric changes of two blocks under 12 treatments (Upper panels for the colonized rock surface, lower panels for the non-colonized rock surface. O: lamp on, A: lamp on and off, F: lamp off).

Figure 9. Relationships between median values of 2-hourly microtopographic changes and each environmental factor for 12 different treatments. Linear trend lines for each observation are shown (Upper panels for the colonized rock surface, lower panels for the non-colonized rock surface. O: lamp on, A: lamp on and off, F: lamp off).

Figure 10. Commonly observed rock fragments caused by spalling around a TMEM bolt set on the supratidal cliff, Marengo. The distance between two bolts is 160 mm.